processes

MDPI

Article

Effects of Catalysts and Membranes on the Performance of Membrane Reactors in Steam Reforming of Ethanol at Moderate Temperature

Manabu Miyamoto [1,*], Yuki Yoshikawa [2], Yasunori Oumi [3], Shin-ichi Yamaura [4] and Shigeyuki Uemiya [1,*]

1 Department of Chemistry and Biomolecular Science, Gifu University, 1-1 Yanagido Gifu 501-1193, Japan
2 Department of Materials Science and Technology, Gifu University, 1-1 Yanagido Gifu 501-1193, Japan; yukiy0115@yahoo.co.jp
3 Division of Instrument Analysis, Life Science Research Center, Gifu University, 1-1 Yanagido Gifu 501-1193, Japan; oumi@gifu-u.ac.jp
4 Institute for Materials Research, Tohoku University, 2-1-1 Katahira, Aoba, Sendai 980-8577, Japan; yamaura@imr.tohoku.ac.jp
* Correspondence: m_miya@gifu-u.ac.jp (M.M.); uemiya@gifu-u.ac.jp (S.U.); Tel./Fax: +81-58-293-2588 (M.M.); +81-58-293-2583 (S.U.)

Academic Editors: Angelo Basile and Catherine Charcosset
Received: 20 April 2016; Accepted: 26 May 2016; Published: 3 June 2016

Abstract: Steam reforming of ethanol in the membrane reactor using the $Pd_{77}Ag_{23}$ membrane was evaluated in Ni/CeO_2 and Co/CeO_2 at atmospheric pressure. At 673 K, the H_2 yield in the $Pd_{77}Ag_{23}$ membrane reactor over Co/CeO_2 was found to be higher than that over Ni/CeO_2, although the H_2 yield over Ni/CeO_2 exceeded that over Co/CeO_2 at 773 K. This difference was owing to their reaction mechanism. At 773 K, the effect of H_2 removal could be understood as the equilibrium shift. In contrast, the H_2 removal kinetically inhibited the reverse methane steam reforming at low temperature. Thus, the low methane-forming reaction rate of Co/CeO_2 was favorable at 673 K. The addition of a trace amount of Ru increased the H_2 yield effectively in the membrane reactor, indicating that a reverse H_2 spill over mechanism of Ru would enhance the kinetical effect of H_2 separation. Finally, the effect of membrane performance on the reactor performance by using amorphous alloy membranes with different compositions was evaluated. The H_2 yield was set in the order of H_2 permeation flux regardless of the membrane composition.

Keywords: amorphous alloy membranes; membrane reactor; steam reforming; ethanol

1. Introduction

Hydrogen has been considered as one of the most promising clean energies because its combustion emits only water. Most of the hydrogen produced currently comes from catalytic steam reforming of natural gas [1]. Steam reforming of natural gas is a mature technology as a practical application, and it has been employed for hydrogen production from various hydrogen sources such as liquefied petroleum gas [2,3] *iso*-octane [4] and kerosene [5–8]. Considering the sustainable society, hydrogen production from fossil fuels is undesirable, and it would shift to renewable sources such as biomass-derived fuels. In particular, biomass-derived liquid fuels are preferable to direct hydrogen storage for on-site hydrogen production owing to their convenience for storage and transport. Among biomass-derived liquid fuels, bioethanol has been frequently studied for hydrogen production because it is easy to handle and distribute and it is readily available [9]. This process can be realized under far milder conditions than those of methane steam reforming. Therefore, the steam reforming of bioethanol is more attractive from practical and environmental view points. In the last decade, many researchers have made efforts to develop catalysts for steam reforming of ethanol aimed at hydrogen production [10–12]. Noble metal catalysts (Pd, Pt, Rh, Ru) exhibited high catalytic activity and stability [13–15]. Inexpensive catalysts involving Ni or Co have been also proposed as appropriate candidates in terms of activity and selectivity [16–19]. However, the process efficiency for hydrogen production must be further improved when hydrogen can be used as an energy source for fuel cells. Additionally, extremely purified hydrogen is required for the low-temperature fuel cells such as proton exchange membrane fuel cells because of irreversible catalyst poisoning even by a trace amount of CO [20,21].

Membrane reactors using hydrogen selective membranes such as Pd and Pd alloy membranes are expected to be one of the promising technologies to achieve high hydrogen production efficiency with high hydrogen purity, because extremely purified hydrogen can be obtained in one step with high hydrogen yield over the thermodynamic equilibrium, owing to simultaneous hydrogen separation from the reaction zone. Therefore, hydrogen production from several fuels using membrane reactors have been extensively studied so far [22–24]. Recently, steam reforming of ethanol has been also investigated by several research groups [25–30]. Basile and co-workers systematically investigated the performance of a membrane reactor using a Pd-Ag membrane packed with Co/Al_2O_3 catalysts in steam reforming of ethanol [25,26], and achieved 100% ethanol conversion, 95.0% CO-free hydrogen recovery and up to 60% CO-free hydrogen yield at 673 K and 3.0 bar. They also investigated the effect of by-products such as acetic acid and glycerol as well [27]. Llorca and co-workers investigated the effect of reactor configurations over Co talc [28] and Co hydrotalcite [29] and demonstrated the higher performance of the catalytic membrane reactors using Pd-Ag membranes compared to the staged membrane reactor, where the catalyst has been placed in-series with the membrane. The enhancement of reactor performance by simultaneous hydrogen separation was also reported by Oyama's group. They evaluated the effect of membrane performance on the reactor performance by comparison between Pd-Cu and SiO_2-Al_2O_3 membranes and found that both permeance and selectivity had a favorable effect on steam reforming of ethanol in membrane reactors [30]. These studies clearly demonstrated the positive effect of membrane reactors in steam reforming of ethanol. However, there are only a few comparison studies on the effect of catalysts and membranes, and, in this study, we evaluated the Pd-Ag membrane reactor packed with Ni or Co based catalysts and then carried out the comparison study of the effect of membranes on the reactor performance using Pd-Ag and amorphous alloy membranes.

2. Experimental Section

2.1. Preparation of Catalysts

For the experiment, 15 wt% Ni/CeO_2 and 15 wt% Co/CeO_2 were prepared as the literature reported [31]. For Ni/CeO_2, nickel acetate tetrahydrate was dissolved in deionized water and stirred at 343 K. After adding CeO_2 (mean particle size: 1 μm), the pH was adjusted to 9 by adding 0.25 M Na_2CO_3 aqueous solution. Then, the water was slowly vaporized at 373 K to obtain the precipitation, and the precipitation was calcined at 673 K for 5 h. For preparation of Co/CeO_2, the preparation procedure was the same to that for Ni/CeO_2. Cobalt acetate tetrahydrate was used as the cobalt source.

Preparation of Ru-Co/CeO_2 and Pd-Co/CeO_2 was as follows. Ruthenium chloride or palladium chloride was dissolved in deionized water and stirred. Then, Co/CeO_2 was added in the solution (M/Co = 0.003 *w*/*w*, M = Ru or Pd) and the solvent was slowly vaporized at 373 K. The obtained solid material was calcinced at 823 K under an N_2 flow for 5 h.

2.2. Preparation of Amorphous Alloy Membranes

Alloy ingots were prepared by arc melting a mixture of pure metals with the appropriate composition. After remelting the alloys several times to make better homogeneity, a ribbon sample was obtained by a single roller melt-spinning method. Both surfaces of the ribbon were polished and sputtered with Pd coating with the thickness of approximately 100 nm. The appearance of obtained membrane was shown in Figure 1.

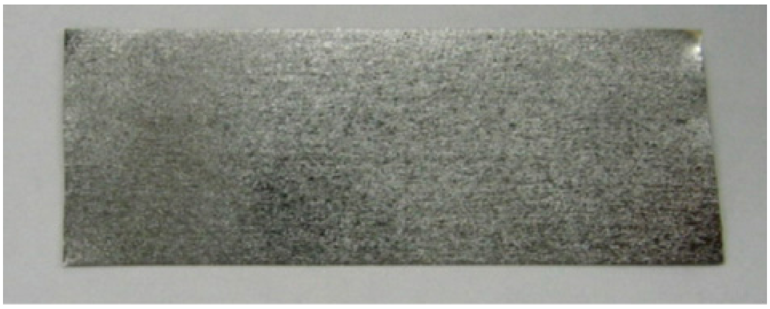

Figure 1. Image of amorphous alloy membrane prepared by single roller melting-spinning method.

2.3. Characterization

Hydrogen permeation tests. The amorphous alloy membranes (size: 10 mm × 10 mm) were placed in the separator sealed by Cu gaskets. The membrane was pre-heated in vacuum up to 673 K. Then, the membrane was cooled down to 623 K. After keeping the membrane at 673 K, H_2 was introduced at the appropriate pressure (0.05, 0.10 and 0.15 MPa-G). The flow rate at the permeation side was measured by the soup-film flow meter.

Catalytic tests. The steam reforming of ethanol was carried out in a conventional reactor and membrane reactor. In the conventional reactor, the 10 g of catalysts was placed in the reactor and heated to 773 K under an N_2 flow. Then, the catalyst was reduced under an H_2 flow at 773 K for 1 h. After controlling the reaction temperature (623–773 K), a mixture of water and ethanol with the steam to carbon ratio (S/C) of two was fed into the reactor at atmospheric pressure. The products were analyzed with a GC-8A gas chromatograph (Shimadzu Corporation, Kyoto, Japan) and the outlet gas flow rate was measured by the soup-film flow meter.

In the membrane reactor, the catalysts and membrane were placed in the reactor. The reactor was heated to 773 K under an N_2 flow, and catalyst was reduced for 1 h under an H_2 flow. The Ar sweep gas was used at the permeation side in the reactor. A mixture of water and ethanol with the S/C of two was fed into the reactor after staying at the reaction temperature. The total pressure at both feed and permeate sides was maintained at atmospheric pressure. The gas composition in the retentate and permeate side was analyzed with the gas chromatograph and the outlet gas flow rate in both sides was measured by the soup flow meter. A $Pd_{77}Ag_{23}$ membrane (thickness: 20 μm, purchased from Tanaka Kikinzoku Kogyo K.K., Tokyo, Japan) was used as reference.

The conversion of ethanol to C_1 products and H_2 yield was calculated as follows:

$$Conversion\ of\ ethanol\ to\ C_1\ products = \frac{flow\ rate\ of\ CO,\ CO_2\ and\ CH_4\ in\ products}{feed\ rate\ of\ ethanol \times 2},$$

$$H_2 yield = \frac{flow\ rate\ of\ H_2\ in\ products}{feed\ rate\ of\ ethanol \times 6}.$$

Additionally, we defined H_2 removal ratio as follows to compare the membrane reactor performance:

$$H_2\ removal\ ratio\ [\%] = \frac{H_2\ permeation\ flow\ rate\ [mol/min]}{Theoritical\ H_2\ production\ rate\ [mol/min]} \times 100.$$

3. Results and Discussion

3.1. Membrane Reactor Performance Using $Pd_{77}Ag_{23}$ Membrane with Co/CeO_2 and Ni/CeO_2 Catalysts

Figure 2 shows the comparison of reactor performance of the conventional reactor and membrane reactor with the Pd membrane over Co/CeO_2 and Ni/CeO_2 catalysts. In the conventional reactor, Ni/CeO_2 exhibited higher conversion of ethanol to C_1 products compared to Co/CeO_2 catalysts. However, the H_2 yield over Ni/CeO_2 did not exceed those over Co/CeO_2 at the reaction temperatures from 673 to 773 K. Regardless of catalysts, the membrane reactor exhibited higher conversion and H_2 yield than the conventional reactor, but the influence of $Pd_{77}Ag_{23}$ membrane was different between the catalysts. The increase in conversion of ethanol to C_1 products over Ni/CeO_2 by the $Pd_{77}Ag_{23}$ membrane was much higher than those over Co/CeO_2 catalysts, and it achieved more than 90% at 723 K, whereas the conversion was only 65% at 773 K over Co/CeO_2. The H_2 yield over Co/CeO_2 increased by almost 13% regardless of temperature, e.g., 44.4% and 57.8% at 773 K for the conventional reactor and membrane reactor, respectively. In contrast, it was found that the increase in H_2 yield over Ni/CeO_2 was significantly improved with an increase in the reaction temperature (from 27.4% at 673 K to 64.5% at 773 K). These results indicate that the influence of H_2 removal from the reaction zone through the $Pd_{77}Ag_{23}$ membrane was higher over Ni/CeO_2 than Co/CeO_2 at the high reaction temperature. However, Co/CeO_2 was suitable for the membrane reactor at low reaction temperature. Figure 3 shows the selectivity of C_1 products. For Ni/CeO_2, the main product at 673 K was methane (58.1%) and a slight decrease in the methane selectivity was observed (51.1%) in the membrane reactor at this reaction temperature. The methane selectivity was slightly decreased to 41.4% at 773 K in the conventional reactor, and the simultaneous H_2 removal by $Pd_{77}Ag_{23}$ membrane greatly enhanced the CO_2 selectivity with decreasing of the methane selectivity. Furthermore, the membrane reactor showed lower methane selectivity of 25.9% at 773 K. For Co/CeO_2, the main product in the conventional reactor was CO_2 regardless of the reaction temperature and the methane selectivity was very low (28.8% and 18.9% at 673 K and 773 K, respectively) compared to Ni/CeO_2. In the membrane reactor, the methane selectivity was decreased, and it was noting that the decrease in methane selectivity was much higher at 673 K than 773 K in Co/CeO_2. Torres *et al.* reported the difference in reaction path in the steam reforming of ethanol [16], and their reaction scheme is summarized in Scheme 1. In the literature, at high reaction temperature, the steam reforming of ethanol was dominant over both Ni and Co catalysts. However, the reaction path was largely different at the moderated reaction temperature between Ni and Co catalysts. The initial reaction was ethanol dehydrogenation to acetaldehyde over both catalysts. The product selectivity approached the thermodynamic equilibrium in Ni catalysts because of the methane-forming reaction such as ethanol cracking, acetaldehyde decarbonilation and the reverse methane steam reforming. On the other hand, the Co catalysts did not promote such methane-forming reactions and the steam reforming of acetaldehyde was preferably occurred. Considering their reaction scheme, the highly increased H_2 yield over Ni/CeO_2 in the membrane reactor at 773 K was due to the shift of equilibrium by simultaneous H_2 removal through the $Pd_{77}Ag_{23}$ membrane. However, at 673 K, it was easy for Ni/CeO_2 to produce methane and the methane steam reforming would be hardly promoted once methane produced even when H_2 was selectively removed from the reaction zone because the methane steam reforming is kinetically and thermodynamically unfavorable at low temperature. Therefore, the low H_2 yield was owing to the preferential production of methane in both conventional and membrane reactors at low temperature. In contrast, because of the low reaction rate of methane-forming reactions in Co/CeO_2, the $Pd_{77}Ag_{23}$ membrane could remove produced H_2 from the reaction zone before H_2 was consumed by the reverse methane steam reforming. This means the selective H_2 removal through $Pd_{77}Ag_{23}$ membrane kinetically inhibited the methane production, resulting in high H_2 yield at low reaction temperature. Indeed, Seelam *et al.* reported Co/Al_2O_2 that showed high membrane performance at 673 K compared to Ni/ZrO_2 because of high methane selectivity in Ni/ZrO_2 [27], which is consistent with our experimental results.

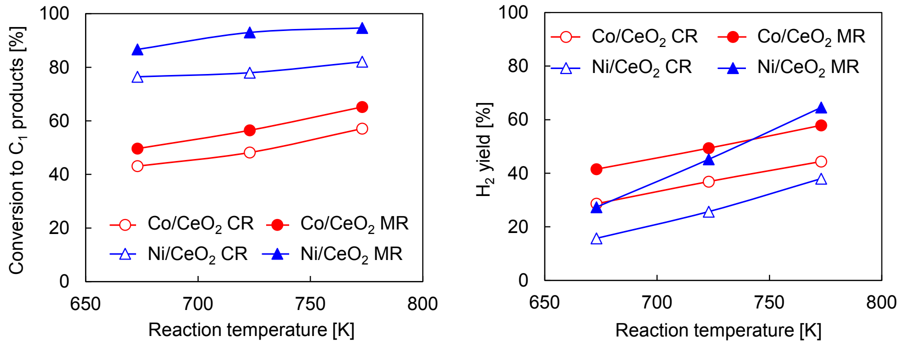

Figure 2. Conversion of ethanol to C_1 products and H_2 yield over Co/CeO_2 and Ni/CeO_2 catalysts in steam reforming of ethanol. CR: conventional reactor, MR: membrane reactor, *W*/*F*: 1.0×10^4 g-cat min/C-mol. $S/C = 2$. Membrane: $Pd_{77}Ag_{23}$, Sweep Ar flow rate: 500 mL/min.

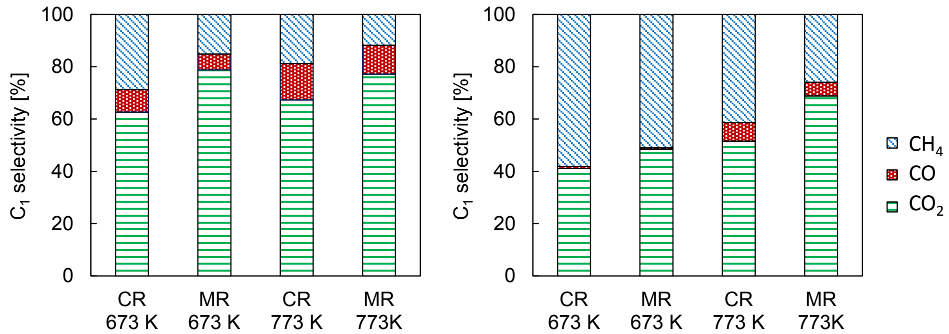

Figure 3. Selectivity of C_1 products over Co/CeO_2 (**left**) and Ni/CeO_2 (**right**) catalysts in steam reforming of ethanol. CR: conventional reactor, MR: membrane reactor, *W*/*F*: 1.0×10^4 g-cat min/C-mol. $S/C = 2$. Membrane: $Pd_{77}Ag_{23}$, Sweep Ar flow rate: 500 mL/min.

High reaction temperature

$C_2H_5OH + H_2O \rightarrow 2CO + 4H_2$ (steam reforming of ethanol)

$CO + H_2O \rightleftharpoons CO_2 + H_2$ (water gas shift)

Low reaction temperature

$C_2H_5OH \rightarrow CH_3CHO + H_2$ (dehydrogenation)

Ni/CeO_2

$\mathbf{CH_3CHO \rightarrow CH_4 + CO}$ **(decarbonilation)**

$\mathbf{CO + 2H_2 \rightleftharpoons CH_4}$ **(reverse methane steam reforming)**

$CO + H_2O \rightleftharpoons CO_2 + H_2$ (water gas shift)

$\mathbf{C_2H_5OH \rightarrow CO + CH_4 + H_2}$ **(Cracking)**

Co/CeO_2

$\mathbf{CH_3CHO + H_2O \rightarrow 2CO + 4H_2}$ **(steam reforming of acetaldehyde)**

$\mathbf{CO + H_2O \rightleftharpoons CO_2 + H_2}$ **(water gas shift)**

Scheme 1. Difference in reaction path over Ni and Co catalysts in steam reforming of ethanol [16].

3.2. Catalyst Development for Improving the Membrane Reactor Performance

Comparing Co/CeO_2 and Ni/CeO_2, Co/CeO_2 was preferable to Ni/CeO_2 for steam reforming of ethanol at low temperature, and the H_2 removal through the $Pd_{77}Ag_{23}$ membrane was very effective at achieving high H_2 yield because of the kinetic inhibition of methane-forming reactions. To improve the membrane reactor performance, we developed the catalysts with addition of a trace amount (M/Co = 0.003 (*w*/*w*)) of precious metals such as Ru and Pd. Table 1 shows the performance of Ru-Co/CeO_2 and Pd-Co/CeO_2 in steam reforming of ethanol in the conventional and membrane reactors. It was interestingly found that the addition of a very small amount of Ru or Pd greatly enhanced the conversion of ethanol to C_1 products. However, the H_2 yield in the conventional reactor was not changed in Ru-Co/CeO_2 and significantly decreased in Pd-Co/CeO_2 compared to Co/CeO_2 (here, it should be noted that the H_2 yield and conversion to C_1 product on Co/CeO_2 was higher than those in Figure 2 even at the same reaction condition. This was owing to the refinement of flow system on the reactor in Figure S1). The low H_2 yield can be explained by the thermodynamic equilibrium. The C_1 selectivity at the thermodynamic equilibrium is CO_2:CO:CH_4 = 30.32:0.15:69.53. Indeed, the methane selectivity approached the thermodynamic value with the increased conversion by the addition of Ru and Pd, resulting in low H_2 yield because produced H_2 was consumed by reverse methane steam reforming from CO_2 and CO. In the membrane reactor, the H_2 yield in both Ru-Co/CeO_2 and Pd-Co/CeO_2 was increased by the simultaneous H_2 separation although the conversion was not changed. In addition, the methane selectivity was decreased by the H_2 removal, and it was much lower than that at the thermodynamic equilibrium as shown in Table 1. This indicates that the H_2 removal by the $Pd_{77}Ag_{23}$ membrane kinetically inhibits the methane-forming reaction but does not shift the equilibrium as mentioned above. The platinum group is well-known to show high H_2 dissociation/association ability and H_2 spillover effect. Otsuka *et al.* reported that Pt accelerated the formation rates of H_2 and CO in the partial oxidation of methane by the reverse spillover of H_2 [32]. Lei *et al.* investigated the effect of Rh in the high temperature water-gas shift reaction, and they found that Rh greatly enhances H_2 release during reoxidation by water, presumably by recombining hydrogen atoms transferred from oxide to metal by reverse spillover [33]. Therefore, the Ru and Pd might accelerate the association of hydrogen atom and desorption of H_2 molecules from the catalyst through the reverse spillover mechanism. Comparing Ru-Co/CeO_2 and Pd-Co/CeO_2, Ru-Co/CeO_2 exhibited high H_2 yield and low methane selectivity. From the investigation in C_1 selectivity with the conversions of ethanol as shown in Figure 4, the methane selectivity in Pd-Co/CeO_2 was increased at lower conversions compared to Ru-Co/CeO_2. This clearly indicates that the promotion effect of methane-forming reaction was higher in Pd than Ru, probably caused by high H_2 storage capacity of Pd. Thus, the Pd membrane could effectively remove H_2 through the reverse spillover on Ru before they reacted with CO_2 or CO to methane, resulting in higher H_2 yield in Ru-Co/CeO_2. On the other hand, a certain part of hydrogen would react with CO_2 and CO due to relatively high hydrogen concentration on Pd before desorption of H_2 molecules by the reverse spillover mechanism, although the $Pd_{77}Ag_{23}$ membrane removed H_2 from the reaction zone.

Table 1. Performance of conventional and membrane reactors over Ru-Co/CeO_2 and Pd-Co/CeO_2 in steam reforming of ethanol.

Catalysts		Conversion to C_1 (%)	H_2 Yield (%)	C_1 Selectivity (%)		
				CO_2	CO	CH_4
Co/CeO_2	CR	63.4	47.6	70.3	6.0	23.6
Ru-Co/CeO_2	CR	86.8	42.3	59.0	3.3	37.7
	MR	87.9	70.3	81.8	4.0	14.2
Pd-Co/CeO_2	CR	92.7	30.8	51.6	1.9	46.5
	MR	94.2	52.9	65.3	2.4	32.3

Reaction temperature: 623 K, W/F: 1.0×10^4 g-cat min/C-mol. *S*/*C* = 2. Membrane: $Pd_{77}Ag_{23}$, Sweep Ar flow rate: 500 mL/min. CR: conventional reactor, MR: membrane reactor.

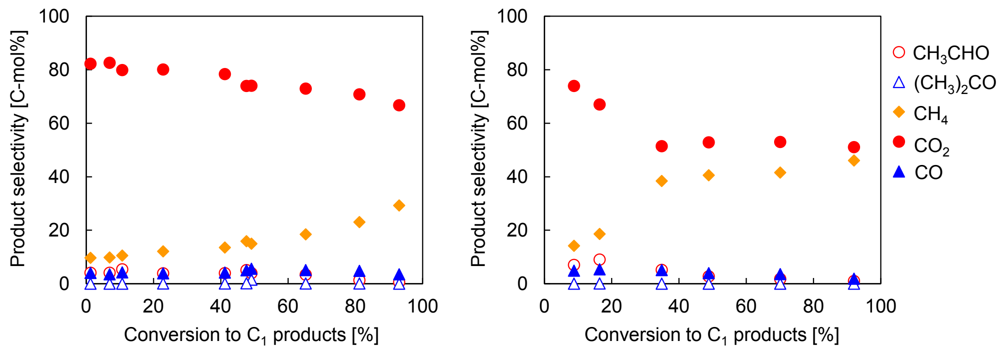

Figure 4. Product distribution over Ru-Co/CeO_2 (**left**) and Pd-Co/CeO_2 (**right**) in steam reforming of ethanol in conventional reactor. Reaction temperature: 623 K, $S/C = 2$.

3.3. *Comparison of Amorphous Alloy Membranes and $Pd_{77}Ag_{23}$ Membrane in the Membrane Reactor*

Figure 5 shows the H_2 permeability of amorphous alloy membranes. The H_2 permeability of Ni-Nb-Zr ternary alloy membrane was increased with increasing Zr content as the literature reported [34,35]. The H_2 permeability of $(Ni_{0.6}Nb_{0.4})_{70}Zr_{30}$ was approximately 8.8×10^{-9} mol·m^{-1}·s^{-1}·Pa$^{-0.5}$, which is consistent with the value reported by the researchers [36]. Paglieri *et al.* reported that the addition of Ta lowered the H_2 permeability, although this slightly improves the thermal stability [37]. We have found that the increase in Ta content slightly decreased the H_2 permeability of Ni-Nb-Ta-Zr quaternary alloy membranes [38]. Indeed, Ni-Ta-Zr ternary alloy membranes showed the lower H_2 permeability in our study as well. In contrast, the addition of a small amount of Zr and Ta increased the H_2 permeability in Nb-Ni-Co alloy membranes because the introduction of larger atoms expanded the amorphous structure, resulting in an increase in H_2 diffusivity [39]. Thus, the $Ni_{40}Nb_{20}Ta_5Zr_{30}Co_5$ alloy membrane exhibited the highest H_2 permeability that was comparable to the $Pd_{77}Ag_{23}$ membrane.

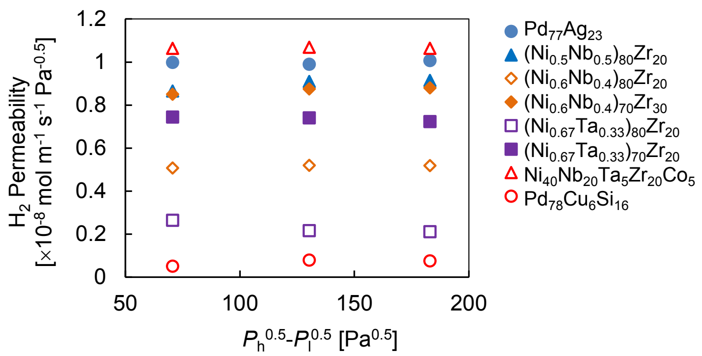

Figure 5. H_2 permeability of amorphous alloy membranes at 623 K. P_h = 0.15, 0.20 and 0.25 MPa.

The steam reforming of ethanol over Ru-Co/CeO_2 was evaluated in the membrane reactors with amorphous alloy membranes. Table 2 summarizes the membrane reactor performance. The H_2 yield was clearly related to H_2 removal ratio. Indeed, the amorphous membranes with the lowest H_2 removal ratio of approximately 10%, such as $(Ni_{0.67}Ta_{0.33})_{80}Zr_{20}$ and $Pd_{78}Cu_6Si_{16}$, exhibited the same membrane reactor performance, and a similar H_2 yield was obtained on the $(Ni_{0.6}Nb_{0.4})_{70}Zr_{30}$ and $Ni_{40}Nb_{20}Ta_5Zr_{30}Co_5$ with the highest H_2 removal ratio of approximately 50%. However, the H_2 removal ratio was not the same order of the H_2 permeability. For example, the H_2 yield and H_2 removal ratio in the $(Ni_{0.6}Nb_{0.4})_{70}Zr_{30}$ membrane was higher than that in the $(Ni_{0.5}Nb_{0.5})_{80}Zr_{20}$ and was almost comparable to $Ni_{40}Nb_{20}Ta_5Zr_{30}Co_5$, although the H_2 permeability was on the order of

$Ni_{40}Nb_{20}Ta_5Zr_{30}Co_5$ > $(Ni_{0.5}Nb_{0.5})_{80}Zr_{20} \cong (Ni_{0.6}Nb_{0.4})_{70}Zr_{30}$. This could be owing to their membrane thickness that is in inverse proportion to the H_2 permeation flux when the membrane is thick enough.

Table 2. Comparison of the membrane reactor performance using amorphous alloy membranes and $Pd_{77}Ag_{23}$ membrane in the steam reforming of ethanol.

Membrane	Membrane Thickness (μm)	H_2 removal (%)	H_2 Yield (%)	C_1 Selectivity (%)		
				CO_2	CO	CH_4
$(Ni_{0.5}Nb_{0.5})_{80}Zr_{20}$	41.6	40.0	58.1	72.9	3.7	23.4
$(Ni_{0.6}Nb_{0.4})_{80}Zr_{20}$	40.6	37.0	57.7	71.8	3.4	24.7
$(Ni_{0.6}Nb_{0.4})_{70}Zr_{30}$	27.7	49.2	65.6	75.8	2.8	21.4
$(Ni_{0.67}Ta_{0.33})_{80}Zr_{20}$	35.7	10.0	47.9	66.3	5.1	29.0
$(Ni_{0.67}Ta_{0.33})_{70}Zr_{30}$	38.7	36.6	55.7	69.3	5.2	25.5
$Ni_{40}Nb_{20}Ta_5Zr_{30}Co_5$	30.4	50.9	67.2	79.0	3.8	17.2
$Pd_{78}Cu_6Si_{16}$	28.1	9.6	46.5	65.8	5.4	28.8
$Pd_{77}Ag_{23}$	20.0	58.0	70.3	81.8	4.0	14.2

Catalyst: Ru-Co/CeO_2, reaction temperature: 623 K, 1.0 × 10^4 g-cat min/C-mol. *S*/*C* = 2, sweep Ar flow rate: 500 mL/min.

Finally, we carried out the steam reforming of ethanol in the $Pd_{77}Ag_{23}$ membrane reactor with different sweep Ar flow rate to understand the effect of H_2 removal by the membrane on H_2 yield. Figure 6 shows the H_2 yield and C_1 selectivity as a function of H_2 removal ratio. The solid lines were interpolated from the experimental results on the $Pd_{77}Ag_{23}$ membrane reactor by varying the sweep Ar flow rate to obtain different H_2 removal ratio. Interestingly, the H_2 yield and C_1 selectivity in the amorphous membranes fitted the curve well. This clearly shows that the membrane reactor performance was determined by the H_2 removal ratio. Considering the reaction mechanism mentioned in Section 3.1, at the low reaction temperature, the catalytic performance such as C_1 selectivity was kinetically controlled by the H_2 permeation rate through the membrane. Thus, it is not an unexpected result that the membrane reactor performance using different amorphous membranes fitted those with the $Pd_{77}Ag_{23}$ membrane. In other words, we can roughly predict the membrane reactor performance based on their actual H_2 permeation flux regardless of the metal composition of the alloy membranes. Indeed, the H_2 removal ratio is clearly related to the H_2 permeation flux of the membrane as shown in Figure 7.

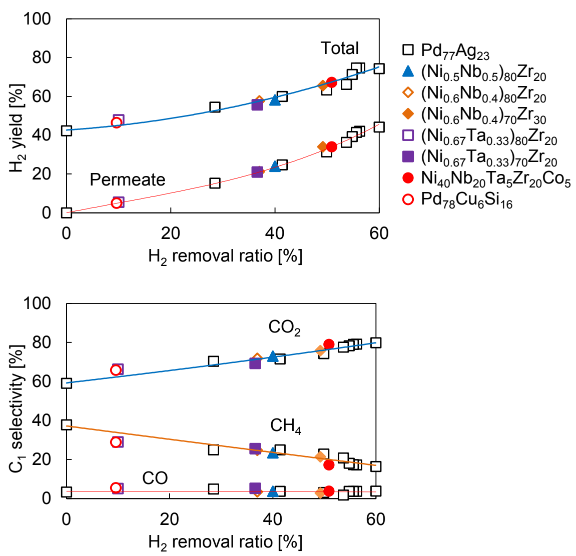

Figure 6. H_2 yield and C_1 selectivity in the membrane reactors using $Pd_{77}Ag_{23}$ and amorphous alloy membranes in steam reforming of ethanol at 623 K. Catalyst: Ru-Co/CeO_2, 1.0 × 10^4 g-cat min/C-mol. *S*/*C* = 2.

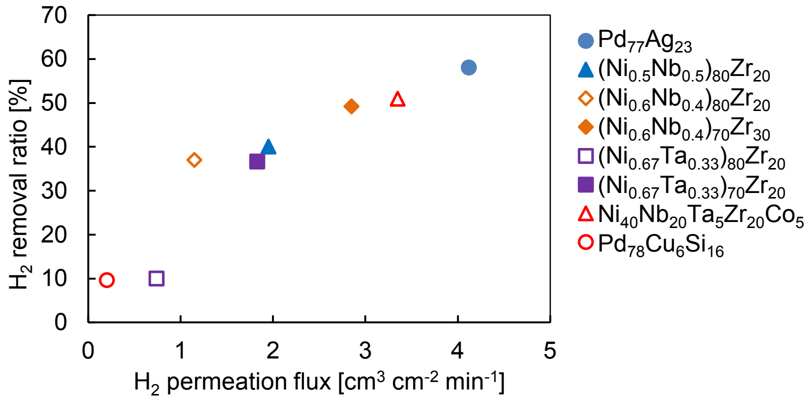

Figure 7. H_2 removal ratio as a function of H_2 permeation flux in the amorphous alloy membranes and $Pd_{77}Ag_{23}$ membrane at 623 K and 0.05 MPa-G in the feed side.

4. Conclusions

We evaluated the Pd membrane performance over Ni/CeO_2 and Co/CeO_2 in steam reforming of ethanol. In the conventional fixed bed reactor, Ni/CeO_2 showed low H_2 yield compared to Co/CeO_2 although the conversion to C_1 products was much higher at the temperatures. In the membrane reactor, the simultaneous H_2 separation improved both conversion of ethanol to C_1 products and H_2 yield. For Ni/CeO_2, the H_2 yield exceeded that in Co/CeO_2 at 773 K. However, at 673 K, although H_2 yield over Ni/CeO_2 was slightly increased by H_2 removal, it was lower than that over Co/CeO_2. The difference of the H_2 removal effect in those catalysts could be due to their reaction mechanism. At high reaction temperature, the higher the reaction rate of steam reforming of ethanol in Ni/CeO_2 compared to Co/CeO_2, the higher the increase rate of H_2 yield that was achieved due to the higher equilibrium shift effect by H_2 removal. However, at low reaction temperature, the methane-forming reaction in Ni/CeO_2 inhibits the H_2 permeation, resulting in a low H_2 yield. From these results, the H_2 separation membrane can improve the H_2 yield thermodynamically at high reaction temperature, but the simultaneous H_2 separation kinetically inhibited methane formation by H_2 removal at a low reaction temperature.

The amorphous alloy membranes with different compositions were employed in the steam reforming of ethanol, and the membrane reactor performance was compared with the $Pd_{77}Ag_{23}$ membrane. Regardless of membrane composition, the membrane reactor performance could be set in the order of H_2 permeation flux.

Acknowledgments: This work was performed under the inter-university cooperative research program(Proposal No. 10G0045) of the Advanced Research Center of Metallic Glasses, Institute for materials Research, Tohoku University

Author Contributions: M.M. and S.U. conceived and designed the experiments; Y.Y. performed the experiments and analyzed the data; Y.O. contributed analysis tools; S.Y. provided the amorphous membranes; M.M. wrote the paper.

Conflicts of Interest: The authors declare no conflict of interest.

References

1. Holladay, J.D.; Hu, J.; King, D.L.; Wang, Y. An overview of hydrogen production technologies. *Catal. Today* **2009**, *139*, 244–260. [CrossRef]
2. Zou, X.; Wang, X.; Li, L.; Shen, K.; Lu, X.; Ding, W. Development of highly effective supported nickel catalysts for pre-reforming of liquefied petroleum gas under low steam to carbon molar ratios. *Int. J. Hydrogen Energy* **2010**, *35*, 12191–12200. [CrossRef]
3. Laosiripojana, N.; Assabumrungrat, S. Hydrogen production from steam and autothermal reforming of LPG over high surface area ceria. *J. Power Sources* **2006**, *158*, 1348–1357. [CrossRef]

4. Lu, Y.; Chen, J.; Liu, Y.; Xue, Q.; He, M. Highly sulfur-tolerant Pt/$Ce_{0.8}Gd_{0.2}O_{1.9}$ catalyst for steam reforming of liquid hydrocarbons in fuel cell applications. *J. Catal.* **2008**, *254*, 39–48. [CrossRef]
5. Suzuki, T.; Iwanami, H.; Yoshinari, T. Steam reforming of kerosene on Ru/Al_2O_3 catalyst to yield hydrogen. *Int. J. Hydrogen Energy* **2000**, *25*, 119–126. [CrossRef]
6. Yu, X.H.; Zhang, S.C.; Wang, L.Q.; Jiang, Q.; Li, S.G.; Tao, Z. Hydrogen production from steam reforming of kerosene over Ni-La and Ni-La-K/cordierite catalysts. *Fuel* **2006**, *85*, 1708–1713. [CrossRef]
7. Muramoto, T.; Nariai, K.; Ohara, H.; Kamata, H. Durability of Ru/CeO_2/γ-Al_2O_3 catalyst for steam reforming of dodecane. *J. Jpn. Petrol. Inst.* **2009**, *52*, 108–113. [CrossRef]
8. Miyamoto, M.; Arakawa, M.; Oumi, Y.; Uemiya, S. Influence of metal cation doping on Ru/CeO_2/Al_2O_3 catalyst for steam reforming of desulfurized kerosene. *Int. J. Hydrogen Energy* **2015**, *40*, 2657–2662. [CrossRef]
9. Murdoch, M.; Waterhouse, G.I.N.; Nadeem, M.A.; Metson, J.B.; Keane, M.A.; Howe, R.F.; Llorca, J.; Idriss, H. The effect of gold loading and particle size on photocatalytic hydrogen production from ethanol over Au/TiO_2 nanoparticles. *Nat. Chem.* **2011**, *3*, 489–492. [CrossRef] [PubMed]
10. Meng, N.; Leung, D.Y.C.; Leung, M.K.H. A review on reforming bio-ethanol for hydrogen production. *Int. J. Hydrogen Energy* **2007**, *32*, 3238–3247.
11. Vaidya, P.D.; Rodrigues, A.E. Insight into steam reforming of ethanol to produce hydrogen for fuel cells. *Chem. Eng. J.* **2006**, *117*, 39–49. [CrossRef]
12. Haryanto, A.; Fernando, S.; Murali, N.; Adhikari, S. Current status of hydrogen production techniques by steam reforming of ethanol: A Review. *Energy & Fuel* **2005**, *19*, 2098–2106.
13. Deluga, G.A.; Salge, J.R.; Schmidt, L.D.; Verykios, X.E. Renewable hydrogen from ethanol by autothermal reforming. *Science* **2004**, *303*, 993–997. [CrossRef] [PubMed]
14. Frusteri, F.; Freni, S. Bio-ethanol, a suitable fuel to produce hydrogen for a molten carbonate fuel cell. *J. Power Source* **2007**, *173*, 200–209. [CrossRef]
15. Idriss, H.; Scott, M.; Llorca, J.; Chan, S.C.; Chiu, W.; Sheng, P.-Y.; Yee, A.; Blackford, M.A.; Pas, S.J.; Hill, A.J.; *et al.* A Phenomenological study of the metal–oxide interface: The role of catalysis in hydrogen production from renewable resources. *ChemSusChem* **2008**, *1*, 905–910. [CrossRef] [PubMed]
16. Torres, J.A.; Llorca, J.; Casanovas, A.; Domínguez, M.; Salvadó, J.; Montané, D. Steam reforming of ethanol at moderate temperature: Multifactorial design analysis of Ni/La_2O_3-Al_2O_3 and Fe- and Mn-promoted Co/ZnO catalysts. *J. Power Source* **2007**, *169*, 158–166. [CrossRef]
17. Sun, J.; Qiu, X.-P.; Wu, F.; Zhu, W.-T. H_2 from steam reforming of ethanol at low temperature over Ni/Y_2O_3, Ni/La_2O_3 and Ni/Al_2O_3 catalysts for fuel-cell application. *Int. J. Hydrogen Energy* **2005**, *30*, 437–445. [CrossRef]
18. Comas, J.; Mariño, F.; Laborde, M.; Amadeo, N. Bio-ethanol steam reforming on Ni/Al_2O_3 catalyst. *Chem. Eng. J.* **2004**, *98*, 61–68. [CrossRef]
19. Casanovas, A.; de Leitenburg, C.; Trovarelli, A.; Llorca, J. Catalytic monoliths for ethanol steam reforming. *Catal. Today* **2008**, *138*, 187–192. [CrossRef]
20. Rikukawa, M.; Sanui, K. Proton-conducting polymer electrolyte membranes based on hydrocarbon polymers. *Prog. Polym. Sci.* **2000**, *25*, 1463–1502. [CrossRef]
21. Neburchilov, V.; Martin, J.; Wang, H.; Zhang, J. A review of polymer electrolyte membranes for direct methanol fuel cells. *J. Power Sources* **2007**, *169*, 221–238. [CrossRef]
22. Rakib, M.A.; Grace, J.R.; Lim, C.J.; Elnashaie, S.S.E.H.; Ghiasi, B. Steam reforming of propane in a fluidized bed membrane reactor for hydrogen production. *Int. J. Hydrogen Energy* **2010**, *35*, 6276–6290. [CrossRef]
23. Perna, A.; Cicconardi, S.P.; Cozzolino, R. Performance evaluation of a fuel processing system based on membrane reactors technology integrated with a PMFC stack. *Int. J. Hydrogen Energy* **2011**, *36*, 9906–9915. [CrossRef]
24. Miyamoto, M.; Hayakawa, C.; Kamata, K.; Arakawa, M.; Uemiya, S. Influence of the pre-reformer in steam reforming of dodecane using a Pd alloy membrane reactor. *Int. J. Hydrogen Energy* **2011**, *36*, 7771–7775. [CrossRef]
25. Iulianelli, A.; Basile, A. An experimental study on bio-ethanol steam reforming in a catalytic membrane reactor. Part I: Temperature and sweep-gas flow configuration effects. *Int. J. Hydrogen Energy* **2010**, *35*, 3170–3177. [CrossRef]

26. Iulianelli, A.; Liguori, S.; Longo, T.; Tosti, S.; Pinacci, P.; Basile, A. An experimental study on bio-ethanol steam reforming in a catalytic membrane reactor. Part II: Reaction pressure, sweep factor and WHSV effects. *Int. J. Hydrogen Energy* **2010**, *35*, 3159–3164. [CrossRef]
27. Seelam, P.K.; Liguori, S.; Iulianelli, A.; Pinacci, P.; Calabrò, V.; Huuhtanen, M.; Keiski, R.; Piemonte, V.; Tosti, S.; De Falco, M.; *et al.* Hydrogen production from bio-ethanol steam reforming reaction in a Pd/PSS membrane reactor. *Catal. Today* **2012**, *193*, 42–48. [CrossRef]
28. Domínguez, M.; Taboada, E.; Molins, E.; Llorca, J. Ethanol steam reforming at very low temperature over cobalt talc in a membrane reactor. *Catal. Today* **2012**, *139*, 101–106. [CrossRef]
29. Espinal, R.; Anzola, A.; Adrover, E.; Roig, M.; Chimentao, R.; Medina, F.; López, E.; Borio, D.; Llorca, J. Durable ethanol steam reforming in a catalyticmembrane reactor at moderate temperature over cobalt hydrotalcite. *Int. J. Hydrogen Energy* **2014**, *39*, 10902–10910. [CrossRef]
30. Lim, H.; Gu, Y.; Oyama, S.T. Studies of the effect of pressure and hydrogen permeance on the ethanol steam reforming reaction with palladium- and silica-based membranes. *J. Membr. Sci.* **2012**, *396*, 119–127. [CrossRef]
31. Zhang, B.; Tang, X.; Li, Y.; Xu, Y.; Shen, W. Hydrogen production from steam reforming of ethanol and glycerol over ceria-supported metal catalysts. *Int. J. Hydrogen Energy* **2007**, *32*, 2367–2373. [CrossRef]
32. Otsuka, K.; Wang, Y.; Sunada, E.; Yamanaka, I. Direct partial oxidation of methane to synthesis gas by cerium oxide. *J. Catal.* **1998**, *175*, 152–160. [CrossRef]
33. Lei, Y.; Cant, N.W.; Trimm, D.L. The origin of rhodium promotion of Fe_3O_4–Cr_2O_3 catalysts for the high-temperature water–gas shift reaction. *J. Catal.* **2006**, *239*, 227–236. [CrossRef]
34. Yamaura, S.; Sakurai, M.; Hasegawa, M.; Wakoh, K.; Shimpo, Y.; Nishida, M.; Kimura, H.; Matsubara, E.; Inoue, A. Hydrogen permeation and structural features of melt-spun Ni–Nb–Zr amorphous alloys. *Acta Mater.* **2005**, *53*, 3703–3711. [CrossRef]
35. Yamaura, S.; Shimpo, Y.; Okouchi, H.; Nishida, M.; Kajita, O.; Kimura, H.; Inoue, A. Hydrogen permeation characteristics of melt-spun Ni–Nb–Zr amorphous alloy membranes. *Matar. Trans.* **2003**, *44*, 1885–1890. [CrossRef]
36. Kim, S.-M.; Chandra, D.; Pal, N.K.; Dolan, M.D.; Chien, W.-M.; Talekar, A.; Lamb, J.; Paglieri, S.N.; Flanagan, T.B. Hydrogen permeability and crystallization kinetics in amorphous Ni-Nb-Zr alloys. *Int. J. Hydrogen Energy* **2012**, *37*, 3904–3913. [CrossRef]
37. Paglieri, S.N.; Pal, N.K.; Dolan, M.D.; Kim, S.-M.; Chien, W.-M.; Lamb, J.; Chandra, D.; Hubbard, K.M.; Moore, D.P. Hydrogen permeability, thermal stability and hydrogen embrittlement of Ni–Nb–Zr and Ni–Nb–Ta–Zr amorphous alloy membranes. *J. Membr. Sci.* **2011**, *378*, 42–50. [CrossRef]
38. Qiang, J.B.; Zhang, W.; Yamaura, S.; Inoue, A. Thermal stability and hydrogen permeation of $Ni_{42}Zr_{30}Nb_{28\text{-}x}Ta_x$ amorphous alloys. *Matar. Trans.* **2009**, *50*, 1236–1239. [CrossRef]
39. Ding, H.Y.; Zhang, W.; Yamaura, S.; Yao, K.F. Hydrogen permeable Nb-based amorphous alloys with high thermal stability. *Mater. Trans.* **2013**, *54*, 1330–1334. [CrossRef]